Inorganic Chemistry

ARTICLE

pubs.acs.org/IC

Mechanochromic Luminescence Switch of Platinum(II) Complexes with 5-Trimethylsilylethynyl-2,2′-bipyridine

Jun Ni,[†,‡] Xu Zhang,[†] Nan Qiu,[§] Yu-Hui Wu,[†] Li-Yi Zhang,[†] Jing Zhang,*[,§] and Zhong-Ning Chen*[,†]

[†]State Key Laboratory of Structural Chemistry, Fujian Institute of Research on the Structure of Matter, Chinese Academy of Sciences, Fuzhou, Fujian 350002, China

[‡]College of Chemistry, Dalian University of Technology, Dalian, Liaoning 116023, China

[§]Synchrotron Radiation Laboratory, Institute of High Energy Physics, Chinese Academy of Science, Beijing 100039, China

Supporting Information

ABSTRACT: Planar platinum(II) complexes Pt(bpyC≡CSiMe$_3$)(C≡CC$_6$H$_4$R-4)$_2$ (R = H (**1**), Bu^t (**2**)) with 5-trimethylsilylethynyl-2,2′-bipyridine show an unusual, reversible, and reproducible mechanical stimuli-responsive color and luminescence switch. When crystalline **1** or **2** is ground, bright yellow-green emitting is immediately converted to red luminescence with an emission red shift of 121−155 nm for **1** or 53−89 nm for **2**. Meanwhile, the crystalline state is transformed to an amorphous phase that can be reverted to the original crystalline state by organic vapor adsorbing or heating, along with red luminescence turning back to yellow-green emitting. The reversibility and reproducibility of luminescence mechanochromic properties have been dynamically monitored by the variations in emission spectra and X-ray diffraction patterns. The drastic grinding-triggered emission red shift is likely involved in the formation of a dimer or an aggregate through Pt−Pt interaction, resulting in a conversion of the ^{3}MLCT/^{3}LLCT emissive state in the crystalline state into the ^{3}MMLCT triplet state in the amorphous phase. Compared with the drastic grinding-triggered emission red shift in **1** (121−155 nm), the corresponding response shift in **2** (53−89 nm) is much smaller since a bulky *tert*-butyl in C≡CC$_6$H$_4$bu^t-4 induces the planar platinum(II) molecules to stack through a longer Pt−Pt distance and less intermetallic contact compared with that in **1**, as suggested from EXAFS studies.

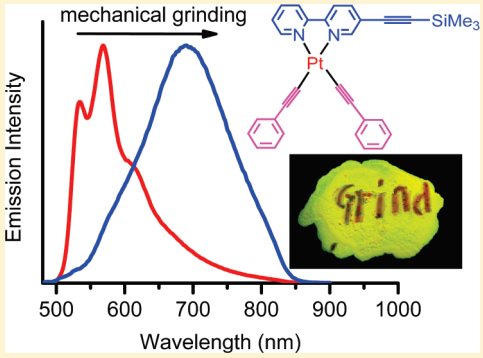

INTRODUCTION

A stimuli-responsive luminescence and color switch is usually associated with a metastable state that is triggered by external stimuli, such as light, electricity, heat, vapor, mechanical force, etc., and can be reverted to the original state by another external signal perturbation.[1] Luminescence mechanochromism is a reversible light-emitting or color switch triggered by mechanical stimuli, such as grinding, crushing, rubbing, extruding, or pressing, and is useful in mechanical sensing, stress monitoring, damage detecting, optical recording, memory, and display.[2,3] A number of organic compounds, including organic dyes,[4] liquid crystals,[5] and polymers,[6] are known to change their absorption and emission characteristics in response to mechanical stimuli. Relevant studies on metal complexes, however, are much less explored, although some metal coordinated species[7−14] have been recently described to show distinct luminescence mechanochromic properties.

It is anticipated that organometallic or coordination compounds composed of both metal ions and organic ligands would exhibit more intriguing and richer luminescence mechanochromism, originating from not only intramolecular conformational folding or twisting but also variation in intermolecular $\pi-\pi$, metal−metal, or hydrogen-bonding interaction. We describe herein a remarkable mechanical grinding-triggered luminescence switch based on bis(σ-phenylacetylide)platinum(II) complexes with 5-trimethylsilylethynyl-2,2′-bipyridine (bpyC≡CSiMe$_3$). A highly reversible and reproducible yellow-green to red luminescence interconversion is achieved by alternate grinding and vapor sorption/heating. Significantly, the mechanoluminescence properties are distinctly alterable by introducing a bulk *tert*-butyl onto the phenylacetylide.

RESULTS AND DISCUSSION

Syntheses and Characterization. Complexes Pt(bpyC≡CSiMe$_3$)(C≡CC$_6$H$_4$R-4)$_2$ (R = H (**1**), Bu^t (**2**)) were prepared by the reaction of Pt(bpyC≡CSiMe$_3$)Cl$_2$ with phenylacetylene or 4-(*tert*-butyl)phenylacetylene in the presence of diisopropylamine and a small amount of CuI. The products are readily purified by chromatography on silica gel columns using dichloromethane as the eluent.

The structures of **1**, **1**·CHCl$_3$, **1**·$^1/_2$CH$_2$ClCH$_2$Cl, and **2**·CH$_2$Cl$_2$ were determined by X-ray crystallography. They exhibit

Received: June 13, 2011
Published: August 03, 2011

some common structural features. The platinum(II) center displays a distorted square-planar geometry composed of C_2N_2 donors. The planar platinum(II) moieties are all arranged in an antiparallel mode for **1**, **1**·$CHCl_3$, **1**·$^1/_2CH_2ClCH_2Cl$, and **2**·CH_2Cl_2, as depicted in Figure 1. There exists a severe sliding between the adjacent platinum(II) moieties so that the shortest Pt···Pt distance is longer than 4 Å, excluding the possibility of intermetallic interaction found in some platinum(II) analogs[15−18] with a stagger stacking pattern that favors formation of a Pt−Pt contact.

Intermolecular C−H···π(C≡C) ($d_{H\cdots C}$ = 2.89 Å, $\theta_{H\cdots C\equiv C}$ = 155.5°) interaction is most likely operating in the structure of **1**. For **1**·$^1/_2CH_2ClCH_2Cl$ (Figure S1, Supporting Information), **1**·$CHCl_3$ (Figure S2, Supporting Information), and **2**·CH_2Cl_2 (Figure S3, Supporting Information), there exist weak interactions between solvate chlorohydrocarbon and platinum(II) moieties, including ClC−H···π(C≡C) ($d_{H\cdots C}$ = 2.63−2.89 Å, $\theta_{H\cdots C\equiv C}$ = 142.0−162.7°) and C−H···ClCH ($d_{H\cdots Cl}$ = 2.86−2.94 Å, $\theta_{C-H\cdots Cl}$ = 121.9 and 172.3°) hydrogen-bonding interactions.

Photophysical Properties. The UV−vis absorption spectra of **1** and **2** (Table 1) in dichloromethane solutions exhibit intense ligand-centered absorption bands at ca. 270, 320, and 345 nm along with a broad low-energy absorption at 427 nm for **1** and 435 nm for **2**, arising likely from dπ(Pt) → π*(bpyC≡CSiMe$_3$) MLCT and π(C≡CC_6H_4R-4) → π*(bpyC≡CSiMe$_3$) (R = H (**1**), Bu^t (**2**)) LLCT states.[19] A distinct red shift of the low-energy absorption band for **2** (Figure S4, Supporting Information) compared with that for **1** is ascribable to the electron-donating character of *tert*-butyl in C≡CC_6H_4Bu^t-4, leading to raise the π(C≡CC_6H_4-R) and dπ(Pt) levels and thus reduce the HOMO−LUMO gap of both MLCT and LLCT transitions for **2**. The broad low-energy band is solvent-dependent and gradually red shifted with the decrease of solvent polarity for both **1** (Figure S5, Supporting Information) and **2** (Figure S6, Supporting Information), revealing an obvious negative solvatochromism.[17a,19] The UV−vis spectra of crystalline species show a broad low-energy band in the near-UV region with the maximum at 425 nm for **1** (Figure 2) and 450 nm for **2** (Figure S7, Supporting Information). Upon grinding, this broad absorption band is obviously red shifted to 446 and 470 nm in the ground samples **1** (Figure 2) and **2** (Figure S7, Supporting Information), respectively.

Upon excitation at λ_{ex} > 350 nm, both **1** and **2** (Figure S4, Supporting Information) are brightly luminescent with a broad emission band centered at 601 nm for **1** and 616 nm for **2** (Table 1) in fluid CH_2Cl_2 solution at ambient temperature. The emission spectra of **1** or **2** are both solvent- and concentration-independent (Figures S5 and S6, Supporting Information). At 77 K in frozen CH_2Cl_2, both **1** (534 and 568 nm) and **2** (547 and 584 sh nm) exhibit vibronic-structured bands with vibrational progressions of around 1250 cm^{-1} (Figures S8 and S9, Supporting Information) as found in solid states. Upon irradiation of crystalline species **1** and **2** at λ_{ex} > 350 nm, both display bright yellow-green luminescence with the lifetime being 0.304 μs for **1** and 0.284 μs for **2** at 298 K. Well-resolved vibronic-structured bands are observed in the emission spectra with vibrational progressional spacings in the range of 1120−1360 cm^{-1} (Table 1), typical of the vibrational frequencies of the aromatic

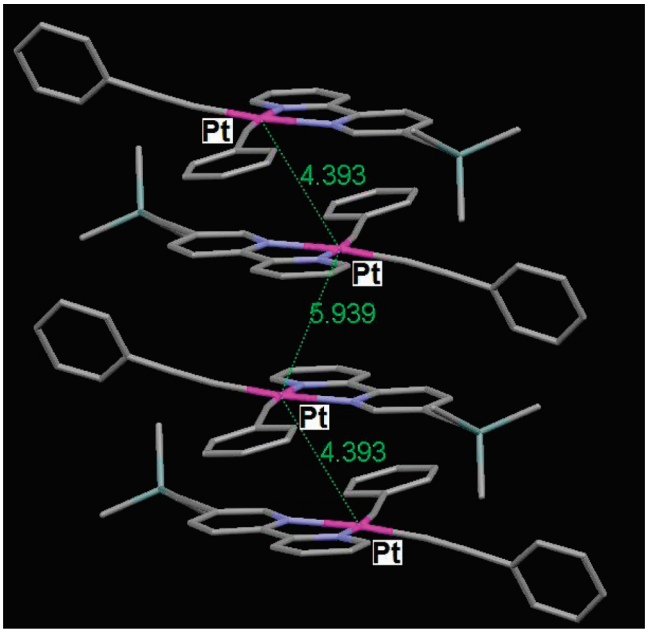

Figure 1. Crystal packing of **1**, showing an antiparallel pattern in stacking of planar platinum(II) molecules with the shortest intermolecular Pt···Pt distances > 4 Å.

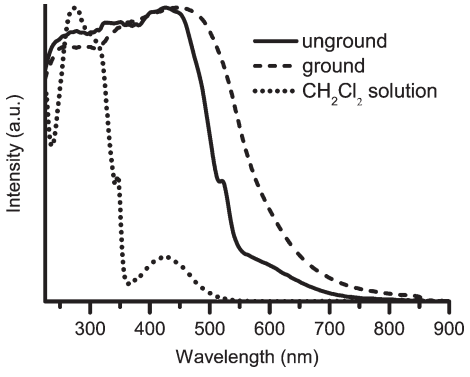

Figure 2. UV−vis spectra of **1** in CH_2Cl_2 solution (dot), crystalline species **1**·$^1/_2CH_2ClCH_2Cl$ (solid), and the ground species (dash).

Table 1. Absorption and Luminescence Data of 1 and 2 at Ambient Temperature

complex	medium	$\lambda_{ab} \times 10^{-3}$ (nm)	λ_{em} (nm)	τ_{em} (μs)	Φ_{em} (%)[a]
1	CH_2Cl_2	275 (39.6), 316 (34.2), 348 (16.3), 427 (6.0)	601	0.120	6.88
	crystalline		535, 569, 614 sh	0.304	
	ground		690	0.080	
2	CH_2Cl_2	275 (56.8), 321 (43.5), 348 (21.5), 435 (7.4)	616	0.091	2.43
	crystalline		529, 565, 612 sh	0.284	
	ground		618	0.100	

[a] The quantum yield in degassed dichloromethane solution was estimated relative to $[Ru(bpy)_3](PF_6)_2$ in acetonitrile as the standard (Φ_{em} = 6.2%).

dx.doi.org/10.1021/ic2012777 |*Inorg. Chem.* 2011, 50, 9090–9096

C═C and C═N modes of the bpyC≡CSiMe$_3$, implying the involvement of bpyC≡CSiMe$_3$ in the emissive state.[19]

Luminescence Mechanochromic Properties. When crystalline species **1** or **2** is ground in an agate mortar or crushed gently on a paper with a spatula, it shows dramatic color and luminescence response with a drastic red shift of the emission band. As depicted in Figure 3 (red), vibronic-structured emission bands at 535 and 569 (614 sh) nm in crystalline species **1** vanish entirely upon mechanical grinding, whereas a broad and unstructured band centered at 690 nm is detected in the thoroughly ground species **1**. Such a mechanical stimuli-responsive red shift of the emission band corresponds to a mechanochromic response shift of 121−155 nm. Meanwhile, bright yellow-green emitting in crystalline species **1** is converted to red luminescence in the ground sample, as indicated in Figure 4. Crystalline species **2** (Figure 3, blue) exhibits well-resolved vibronic-structured emission bands at 529 and 565 (612 sh) nm. Upon mechanical grinding, vibronic-structured emission bands disappear entirely, whereas a red shifted broad and structureless band centered at 618 nm is only observed in the thoroughly ground sample **2**, corresponding to 53−89 nm of luminescence mechanochromic response shift. In contrast strikingly with bright yellow emitting in the crystalline species **2**, the ground sample shows red luminescence (Figure S15, Supporting Information). It is noteworthy that, compared with the grinding-triggered red shift of the emission in **1** (121−155 nm), the corresponding response shift in **2** (53−89 nm) is much smaller, as depicted in Figure 3, implying that introducing a bulky *tert*-butyl onto the phenylacetylide affects significantly the mechanochromic luminescence in **2**.

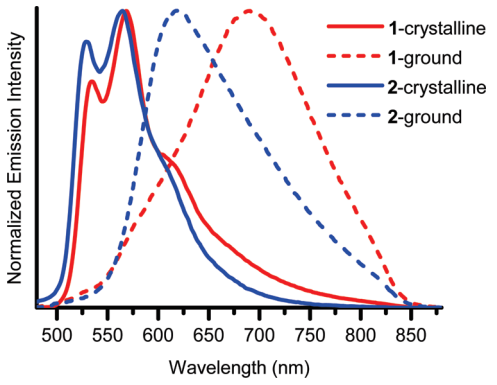

Figure 3. Normalized emission spectra of **1** (red) and **2** (blue) in the crystalline state (solid) and ground state (dash), showing a mechanical grinding-triggered emission red shift of 121−155 nm for **1** and 53−89 nm for **2**.

It is noticeable that the emission spectra of both **1** (Figure S10, Supporting Information) and **2** (Figure S11, Supporting Information) are insensitive to solvate molecules in the crystal structures so that distinct luminescence vapochromism is unobserved. This is quite different from remarkable and selective luminescence vapochromic properties in square-planar platinum(II) complexes with 5,5′-bis(trimethylsilylethynyl)-2,2′-bipyridine (Me$_3$SiC≡CbpyC≡CSiMe$_3$).[13a,15,16] When crystalline species **1**·CHCl$_3$ (Figure S22, Supporting Information) or **2**·CH$_2$Cl$_2$ (Figure S23, Supporting Information) was kept to heat at 120 °C, the emission spectra were not distinctly shifted except some changes in emission intensity. It appears that solvate molecules exert inappreciable influence on the emission spectra of both crystalline and ground species **1** (Figure S12, Supporting Information) or **2** (Figure S13, Supporting Information), although solvate molecules are partially lost in the process of mechanical grinding, as suggested from thermogravimetric analysis studies (Figures S17 and S18, Supporting Information). Therefore, mechanical grinding-triggered color and luminescence changes in the two platinum(II) complexes are not due to loss of the solvent molecules.

Interestingly, the ground species **1** or **2** can be reverted to the original unground state by organic vapor adsorbing or heating. As depicted in Figure 5, the dynamic variation process of the emission spectra was monitored by exposing the ground species **1** to acetone vapor (Figure 5a) or heating at 120 °C (Figure 5b). With gradual attenuation of the unstructured band centered at 690 nm, vibronic-structured bands at 535 and 569 (615 sh) nm occur and grow progressively so as to restore perfectly to the original crystalline state. Figure 4 depicts mechanical grinding-triggered reversible color and luminescence changes for **1** under ambient light and UV light irradiation (365 nm), showing a switch from yellow-green to red upon grinding, and from red turning back to yellow-green when a drop of acetone is added to the ground sample.

X-ray diffraction (XDR) studies on crystalline **1**·CHCl$_3$ and the corresponding ground species (Figure 6) reveal that the XRD patterns disappear entirely upon mechanical grinding (Figure 6,

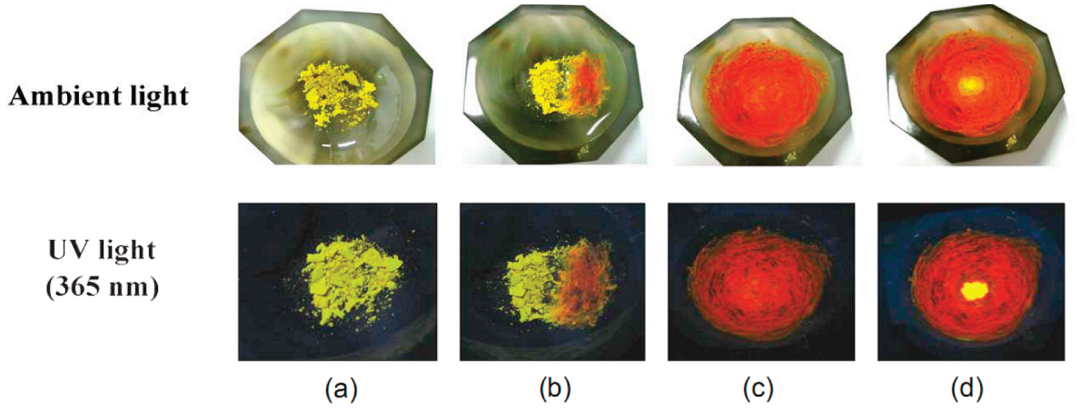

Figure 4. Photographic images of crystalline species **1** in response to mechanical grinding under ambient light and UV light irradiation (365 nm), showing the color and luminescence switches from yellow-green to red upon grinding, and from red turning back to yellow-green by addition of acetone: (a) crystalline sample, (b) partially ground sample, (c) thoroughly ground sample, and (d) ground sample upon addition of a drop of acetone.

dx.doi.org/10.1021/ic2012777 |*Inorg. Chem.* 2011, 50, 9090–9096

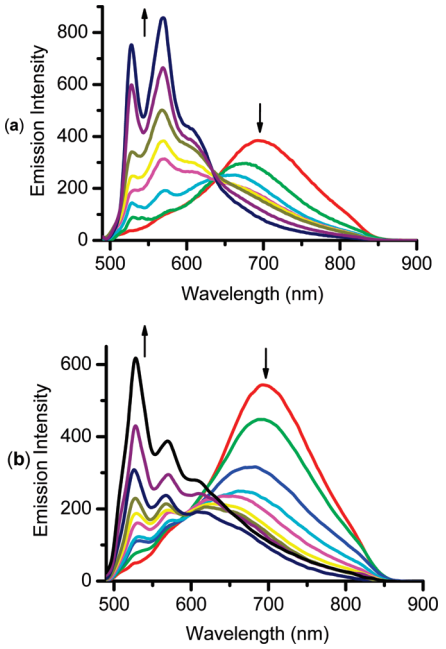

Figure 5. Emission spectral changes of the ground species **1** in response to acetone vapor (a) and heating at 120 °C (b), showing a gradual emission attenuation of the broad unstructured band centered at ca. 690 nm and a progressive emission growing of vibronic-structured bands at ca. 530 and 568 nm.

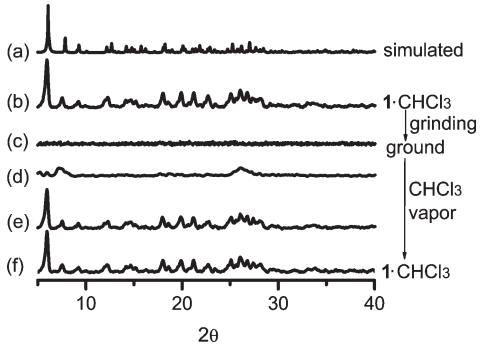

Figure 6. XRD diagrams in a mechanochromic cycle for crystalline species **1**·$CHCl_3$, showing the simulated (a) and measured (b) XRD patterns for the crystalline sample, the measured XRD diagram for the ground sample (c), and dynamic variations (d–f) of the XRD patterns from an amorphous phase to the original crystalline state upon the ground sample being exposed to $CHCl_3$ vapor.

diagram c), implying a conversion from the crystalline state to the amorphous phase when the sample is thoroughly mechanically ground. Nevertheless, when the ground sample is exposed into a saturated $CHCl_3$ vapor for some time, the XRD patterns can be perfectly reverted to the original crystalline state. Figure 6 depicts the XRD diagrams in a mechanochromic cycle for **1**·$CHCl_3$, showing dynamic variations in the XRD patterns in response to mechanical grinding as well as $CHCl_3$ vapor in the reversed process. Heating is another feasible approach to make the amorphous phase in the ground species **1** revert to the original crystalline state, as indicated in Figure 7. Thus, XRD studies demonstrate unambiguously that the mechanical grinding-induced color and luminescence switch is due to interconversion

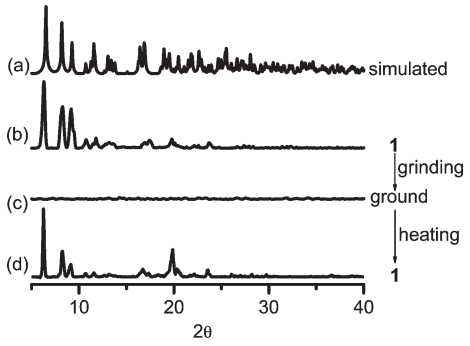

Figure 7. XRD diagrams in a mechanochromic cycle for unsolvated crystalline species **1**, showing the simulated (a) and measured (b) XRD patterns for the crystalline sample, the measured XRD diagram for the ground sample (c), and the reverted XRD patterns (d) by heating the ground sample at 120 °C.

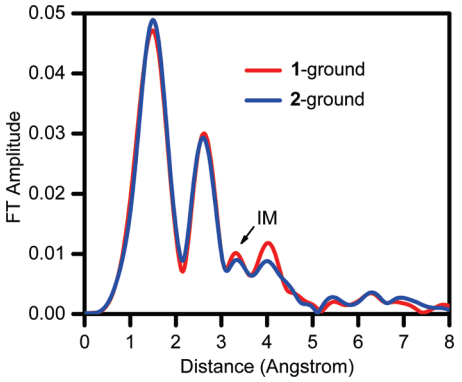

Figure 8. FT spectra of the room-temperature EXAFS results for $k^3\chi(k)$ for the ground samples of **1** (red) and **2** (blue).

between crystalline and amorphous states, which is highly reversible and reproducible.

To elucidate transition characters of the absorption and emission spectra, DFT computational studies were performed on **1** (Tables S1 and S2, Supporting Information) and **2** (Tables S3 and S4, Supporting Information). The HOMO, HOMO-1, and HOMO-2 are contributed by both 5d(Pt) (25.8–42.4% for **1** and 21.7–43.1% for **2**) and $\pi(C{\equiv}CC_6H_4R\text{-}4)$ (52.1–72.1% for **1** and 51.4–75.1% for **2**). The LUMO and LUMO+2 are predominantly resident on $\pi^*(bpyC{\equiv}CSiMe_3)$ (94.1–97.1% for **1** and 94.1–97.3% for **2**). The calculated low-energy singlet absorptions at 516, 481, and 427 nm for **1** (Table S2, Supporting Information) or 530, 497, and 428 nm for **2** (Table S4, Supporting Information) due to HOMO → LUMO, HOMO-1 → LUMO, and HOMO-2 → LUMO transitions, respectively, result primarily from $^1[d\pi(Pt) \rightarrow \pi^*(bpyC{\equiv}CSiMe_3)]$ ^{1}MLCT and $^1[\pi(C{\equiv}CC_6H_4R\text{-}4) \rightarrow \pi^*(bpyC{\equiv}CSiMe_3)]$ (R = H (**1**), But (**2**)) ^{1}LLCT states. The calculated triplet excitation at 552 nm for **1** (Table S2, Supporting Information) or 562 nm for **2** (Table S4, Supporting Information) due to the HOMO → LUMO transition is also typical of the $^3[d\pi(Pt) \rightarrow \pi^*(bpyC{\equiv}CSiMe_3)]$ ^{3}MLCT and $^3[\pi(C{\equiv}CC_6H_4R\text{-}4) \rightarrow \pi^*(bpyC{\equiv}CSiMe_3)]$ ^{3}LLCT triplet excited states.

Upon mechanical grinding, it is likely that the planar platinum(II) molecules are packed in close proximity through Pt–Pt interaction to form a dimer or an aggregate in the amorphous

dx.doi.org/10.1021/ic2012777 |*Inorg. Chem.* 2011, 50, 9090–9096

Table 2. Crystallographic Data for 1, 1·$CHCl_3$, 1·$^1/_2CH_2ClCH_2Cl$, and 2·CH_2Cl_2

	1	1·$CHCl_3$	1·$^1/_2CH_2ClCH_2Cl$	2·CH_2Cl_2
empirical formula	$C_{31}H_{26}N_2PtSi$	$C_{32}H_{27}Cl_3N_2PtSi$	$C_{32}H_{28}ClN_2PtSi$	$C_{40}H_{44}Cl_2N_2PtSi$
formula weight	649.72	769.09	699.19	846.85
crystal system	monoclinic	monoclinic	triclinic	monoclinic
space group	$P2_1/n$	$P2_1/c$	$P\bar{1}$	$P2_1/c$
a, Å	15.716(7)	7.168(3)	7.226(2)	20.480(8)
b, Å	9.145(4)	22.491(8)	13.025(4)	11.270(4)
c, Å	19.615(9)	19.119(7)	16.526(6)	16.377(6)
α, °			79.29(1)	
β, °	103.305(7)	95.463(6)	84.58(1)	93.973(6)
γ, °			74.12(1)	
V, Å^3	2744(2)	3068.2(18)	1468.4(8)	3771(2)
Z	4	4	2	4
ρ_{calcd}, g/cm^{-3}	1.573	1.665	1.581	1.492
μ, mm^{-1}	5.179	4.898	4.932	3.924
radiation (λ, Å)	0.71073	0.71073	0.71073	0.71073
temp, (K)	293(2)	293(2)	293(2)	293(2)
91(F_o)[a]	0.0498	0.0764	0.0618	0.0453
wR2(F_o^2)[b]	0.1133	0.1742	0.1587	0.1178
GOF	1.090	0.993	1.050	1.066

[a] $R1 = \Sigma|F_o - F_c|/\Sigma F_o$. [b] $wR2 = \Sigma[w(F_o^2 - F_c^2)^2]/\Sigma[w(F_o^2)]^{1/2}$.

phase. The emissive state of the ground species is thus converted to the ^{3}MMLCT (metal−metal-to-ligand charge transfer) triplet state involving a HOMO of a dπ^* nature resulting from σ-overlapping between d_{z^2} orbitals of the platinum(II) ions,[18−20] thus giving a much smaller HOMO−LUMO gap and a significantly red shifted emission centered at 690 nm as a broad unstructured band (Figure 3a). Remarkably, the red shift of the emission in **2** (53−89 nm) from crystalline species (529 sh and 565 nm) to the ground species (618 nm) is much less pronounced than that in **1** (121−155 nm). It is probably that the bulky *tert*-butyl of C≡C$C_6H_4Bu^t$-4 in **2** induces the planar platinum(II) molecules to stack through a longer Pt−Pt distance and less intermetallic contact compared with that in **1**, thus inducing a less red shifted mechanochromic luminescence for **2**.

EXAFS studies have been performed to explore the structure information of the ground samples of **1** and **2**. Noticeably, it is difficult to obtain the EXAFS data for the unground samples because very small particles are used in EXAFS measurement, which are usually prepared by grinding the crystalline samples. Figure 8 depicts the Fourier transform (FT) spectra of the room-temperature EXAFS results of the weighted function, $k^3\chi(k)$ for the ground species **1** and **2**. In the first coordination shell of platinum(II), two Pt−C bonds with an average distance of 1.95 Å and two Pt−N bonds with an average distance of 2.07 Å are found in both ground complexes **1** and **2** using a standard least-squares fitting approach. This result coincides well with the bond parameters of **1**, 1·$CHCl_3$, 1·$^1/_2CH_2ClCH_2Cl$, and 2·CH_2Cl_2 from X-ray crystallography. With reference to the previous EXAFS studies on square-planar complexes [Pt(2,2′-bpy)$(SCN)_2$] and [Pt(2,2′-bpy)Cl_2],[21,22] the intermolecular stacking (IM) effects are observable in the range of $r > 2.5$ Å. The FT feature (labeled IM in Figure 8 and falling in the range of $3.0 < R < 3.8$ Å) is associated with intermolecular stacking effects and indicates the formation of the Pt−Pt interactions between adjacent square-planar platinum(II) molecules. Once mechanically ground, both complexes **1** and **2** are likely packed in close proximity through relatively short Pt···Pt separations (<3.5 Å) based on the EXAFS data. Furthermore, the IM feature in **2** is weaker and broader than that in **1**, suggesting that the bulky *tert*-butyl in C≡C$C_6H_4Bu^t$-4 causes a longer intermolecular Pt···Pt distance and a more disordered stacking structure in **2**.

CONCLUSIONS

Square-planar platinum(II) complexes Pt(bpyC≡C$SiMe_3$)-(C≡CC_6H_4R-4)$_2$ (R = H (**1**), Bu^t (**2**)) with 5-trimethylsilylethynyl-2,2′-bipyridine show an unusual, reversible, and reproducible mechanical stimuli-responsive color and luminescence switch. When crystalline species **1** or **2** is ground in an agate mortar or crushed gently on a paper with a spatula, the crystalline state is transformed to an amorphous phase. Meanwhile, bright yellow-green emitting in the crystalline species is immediately converted to red luminescence in the ground sample. Significantly, the amorphous phase in the ground species can be reverted to the original crystalline state by organic vapor adsorbing or heating along with red luminescence turning back to yellow-green emitting. The reversibility and reproducibility of luminescence mechanochromic properties have been dynamically monitored by the variations in emission spectra and X-ray diffraction patterns. The drastic grinding-triggered emission red shift is likely involved in a dimer or an aggregate through Pt−Pt interaction, resulting in a conversion from the ^{3}MLCT/^{3}LLCT emissive state in the crystalline state into the ^{3}MMLCT triplet state in the amorphous phase. Although remarkable luminescence mechanochromic properties occur in both **1** and **2**, introducing a bulky *tert*-butyl onto the phenylacetylide affects significantly the mechanoluminescence in **2**. Compared with the drastic grinding-triggered emission red shift in **1** (121−155 nm), the corresponding response shift in **2** (53−89 nm) is much smaller because the bulky *tert*-butyl of C≡C$C_6H_4Bu^t$-4 in **2** induces planar platinum(II) molecules to stack through a longer Pt−Pt distance and less intermetallic contact compared with that in **1**.

dx.doi.org/10.1021/ic2012777 |*Inorg. Chem.* 2011, 50, 9090–9096

EXPERIMENTAL SECTION

General Procedures and Materials. Synthetic operations were carried out under a dry argon atmosphere using Schlenk techniques and vacuum-line systems unless otherwise specified. The solvents were dried, distilled, and degassed prior to use except that those for spectroscopic measurements were of spectroscopic grade. 5-Trimethylsilylethynyl-2,2′-bipyridine (bpyC≡CSiMe$_3$)[23] and Pt(bpyC≡CSiMe$_3$)Cl$_2$[17] were prepared by the similar synthetic procedures described in the literatures. Other reagents were purchased from commercial sources and used as received unless stated otherwise.

Pt(bpyC≡CSiMe$_3$)(C≡CC$_6$H$_5$)$_2$ (1). To a dichloromethane (50 mL) solution of 1-ethynylbenzene (51.0 mg, 0.5 mmol) were added Pt(bpyC≡CSiMe$_3$)Cl$_2$ (103.6 mg, 0.20 mmol), CuI (1 mg), and diisopropylamine (2 mL) with stirring at ambient temperature for 1 day. The solvents were removed by rotary evaporation, and the product was purified by chromatography on a silica gel column using dichloromethane as the eluent. Yield: 85%. Anal. Calcd for desolvated species $C_{31}H_{26}N_2PtSi$: C, 57.31; H, 4.03; N, 4.31. Found: C, 57.48; H, 4.08; N, 4.27. ESI-MS (m/z): 650.6 $[M + 1]^+$. ^{1}H NMR (400 MHz, $CDCl_3$, ppm): 9.72 (d, 1H, J = 1.6 Hz, bpy), 9.55 (d, 1H, J = 4.8 Hz, bpy), 8.71 (d, 1H, J = 4.8 Hz, bpy), 8.69 (d, 1H, J = 4.8 Hz, bpy), 8.51 (dd, 1H, J = 8.8 Hz, J = 2.0 Hz, bpy), 8.41 (td, 1H, J = 8.0 Hz, J = 1.6 Hz, bpy), 7.91 (t, 1H, J = 6.4 Hz, bpy), 7.27−7.40 (m, 8H, C_6H_5), 7.18−7.24 (m, 2H, C_6H_5), 0.29 (s, 9H, Si(CH_3)$_3$). IR (KBr disk, cm^{-1}): 2114 s (C≡CPt), 2169 m (C≡CSiMe$_3$), 1249 m (Si−C).

Pt(bpyC≡CSiMe$_3$)(C≡CC$_6$H$_4$Bu^t-4)$_2$ (2). This compound was prepared by the same procedure as that of **1** except using 4-(*tert*-butyl)phenylacetylene instead of phenylacetylene. Yield: 82%. Anal. Calcd for $C_{39}H_{42}N_2PtSi$: C, 61.48; H, 5.56; N, 3.68%. Found: C, 61.53; H, 5.66; N, 3.52%. ESI-MS (m/z): 762.8 $[M + 1]^+$. ^{1}H NMR (400 MHz, $CDCl_3$, ppm): 9.53 (d, 1H, J = 4.8 Hz, bpy), 9.51 (d, 1H, J = 1.6 Hz, bpy), 8.15 (t, 2H, J = 8.0 Hz, bpy), 8.04 (dd, 1H, J = 7.2 Hz, J = 2.0 Hz, bpy), 8.00 (td, 1H, J = 7.6 Hz, J = 1.2 Hz, bpy), 7.41−7.46 (m, 1H + 4H, bpy + C_6H_4), 7.28 (t, 4H, J = 8.4 Hz, C_6H_4), 1.33 (s, 9H, C_4H_9), 1.32 (s, 9H, C_4H_9), 0.33 (s, 9H, Si(CH_3)$_3$). IR (KBr disk, cm^{-1}): 2113 s (C≡CPt), 2167 m (C≡CSiMe$_3$), 1250 m (Si−C).

Physical Measurements. Proton NMR spectra were measured on a Bruker Avance III (400 MHz) spectrometer with $SiMe_4$ as the internal reference. UV−vis absorption spectra were measured on a PerkinElmer Lambda 25 UV−vis spectrophotometer. Infrared spectra (IR) were recorded on a Magna 750 FT-IR spectrophotometer with KBr pellets. Elemental analyses (C, H, and N) were carried out on a PerkinElmer model 240 C elemental analyzer. Electrospray ionization mass spectrometry (ESI-MS) was performed on a Finnigan LCQ mass spectrometer using dichloromethane−methanol as mobile phases. Emission and excitation spectra were recorded on a PerkinElmer LS55 luminescence spectrometer with a red-sensitive photomultiplier type R928. Emission lifetimes in solid states and degassed solutions were determined on an Edinburgh analytical instrument (F900 fluorescence spectrometer) using an LED laser at 440 nm excitation. The emission quantum yield (Φ_{em}) in degassed dichloromethane solution at room temperature was calculated by $\Phi_s = \Phi_r(B_r/B_s)(n_s/n_r)^2(D_s/D_r)$ using $[Ru(bpy)_3](PF_6)_2$ in acetonitrile as the standard (Φ_{em} = 0.062), where the subscripts r and s denote reference standard and the sample solution, respectively, and n, D, and Φ are the refractive index of the solvents, the integrated intensity, and the luminescence quantum yield, respectively. The quantity B is calculated by $B = 1-10^{-AL}$, where A is the absorbance at the excitation wavelength and L is the optical path length.

Crystal Structural Determination. Crystals of **1**, **1**·$^1/_2CH_2Cl_2$, **1**·$CHCl_3$, and **2**·CH_2Cl_2 were obtained by layering petroleum ether onto the corresponding solutions. Data collection was performed on a Mercury CCD diffractometer by the ω scan technique at room temperature using graphite-monochromated Mo-Ka (λ = 0.71073 Å) radiation. The CrystalClear software package was used for data reduction and empirical absorption correction. The structures were solved by direct methods. The heavy atoms were located from E-map, and the rest of the non-hydrogen atoms were found in subsequent Fourier maps. All non-hydrogen atoms were refined anisotropically, while the hydrogen atoms were generated geometrically and refined with isotropic thermal parameters. The structures were refined on F_2 by full-matrix least-squares methods using the SHELXTL−97 program package.[24] The crystallographic data are summarized in Table 2.

Theoretical Calculation Methodology. The electronic structures were calculated by density functional theory (DFT)[25] methods using the Gaussian 03 program package.[26] The hybrid functional PBE0[27] was used together with 6-31G(d,p) polarized double-ζ basis sets for C, N, and H atoms and the Stuttgart−Dresden (SDD)[28] basis set with effective core pseudopotentials (ECPs) for the Pt(II) atom. To precisely describe the molecular properties, one additional f-type polarization function was implemented for the platinum(II) atom (α = 0.18).[29] On the basis of the structures, 60 singlet and 6 triplet excited states were obtained to determine the vertical excitation energies for **1** and **2** in dichloromethane, using the time-dependent DFT (TD-DFT) calculations.[30,31] The polarized continuum model method (PCM)[32] with dichloromethane as the solvent was used to calculate all the electronic structures in solution.

ASSOCIATED CONTENT

Supporting Information. Figures giving additional UV−vis and emission spectra, tables and figures giving DFT calculation data, and X-ray crystallographic file in CIF format for the structure determination of compounds **1**, **1**·$CHCl_3$, **1**·$^1/_2CH_2ClCH_2Cl$, and **2**·CH_2Cl_2. This material is available free of charge via the Internet at http://pubs.acs.org.

AUTHOR INFORMATION

Corresponding Author
*E-mail: czn@fjirsm.ac.cn.

ACKNOWLEDGMENT

We acknowledge the financial support from the NSFC (20821061, 20931006, and U0934003), the 973 project (2007CB815304) from MSTC, the NSF of Fujian Province (2008I0027), and the "Fundamental Research Funds for the Central Universities".

REFERENCES

(1) Sagara, Y.; Kato, T. *Nat. Chem.* **2009**, *1*, 605.
(2) Balch, A. L. *Angew. Chem., Int. Ed.* **2009**, *48*, 2641.
(3) Takagi, H. D.; Noda, K.; Itoh, S. *Platinum Met. Rev.* **2004**, *48*, 117.
(4) (a) Asiri, A. M. A.; Heller, H. G.; Hursthouse, M. B.; Karalulov, A. *Chem. Commun.* **2000**, 799. (b) Sagara, Y.; Mutai, T.; Yoshikawa, I.; Araki, K. *J. Am. Chem. Soc.* **2007**, *129*, 1520. (c) Zhang, G.; Lu, J.; Sabat, M.; Fraser, C. L. *J. Am. Chem. Soc.* **2010**, *132*, 2160. (d) Sheth, A. R.; Lubach, J. W.; Munson, E. J.; Muller, F. X.; Grant, D. J. W. *J. Am. Chem. Soc.* **2005**, *127*, 6641. (e) Zhang, G.; Lu, J.; Fraser, C. L. *Inorg. Chem.* **2010**, *49*, 10747.
(5) (a) Kunzelman, J.; Kinami, M.; Crenshaw, B. R.; Protasiewicz, J. D.; Weder, C. *Adv. Mater.* **2008**, *20*, 119. (b) Sagara, Y.; Kato, T. *Angew. Chem., Int. Ed.* **2008**, *47*, 5175. (c) Lawrence, J. R.; Shim, G. H.; Jiang, P.; Han, M. G.; Ying, Y.; Foulger, S. H. *Adv. Mater.* **2005**, *17*, 2344.
(6) (a) Foulger, S. H.; Jiang, P.; Lattam, A. C., Jr.; Smith, D. W.; Ballato, J. *Langmuir* **2001**, *17*, 6023. (b) Crenshaw, B. R.; Burnworth, M.;

Khariwala, D.; Hiltner, A.; Mather, P. T.; Simha, R.; Weder, C. *Macromolecules* **2007**, *40*, 2400.

(7) (a) Lee, Y.-A.; Eisenberg, R. *J. Am. Chem. Soc.* **2003**, *125*, 7778. (b) Schneider, J.; Lee, Y.-A.; Perez, J.; Brennessel, W. W.; Flaschenriem, C.; Eisenberg, R. *Inorg. Chem.* **2008**, *47*, 957.

(8) (a) Assefa, Z.; Omary, M. A.; McBurnett, B. G.; Mohamed, A. A.; Patterson, H. H.; Staples, R. J.; Fackler, J. P. *Inorg. Chem.* **2002**, *41*, 6274. (b) Catalano, V. J.; Horner, S. J. *Inorg. Chem.* **2003**, *42*, 8430.

(9) (a) Ito, H.; Saito, T.; Oshima, N.; Kitamura, N.; Ishizaka, S.; Hinatsu, Y.; Wakeshima, M.; Kato, M.; Tsuge, K.; Sawamura, M. *J. Am. Chem. Soc.* **2008**, *130*, 10044. (b) Kuchison, A. M.; Wolf, M. O.; Patrick, B. O. *Chem. Commun.* **2009**, 7387. (c) Laguna, A.; Lasanta, T.; Lopez-de-Luzuriaga, J. M.; Monge, M.; Naumov, P.; Olmos, M. E. *J. Am. Chem. Soc.* **2010**, *132*, 456. (d) Osawa, M.; Kawata, I.; Igawa, S.; Hoshino, M.; Fukunaga, T.; Hashizume, D. *Chem.—Eur. J.* **2010**, *16*, 12114.

(10) Perruchas, S.; Le Goff, X. F.; Maron, S.; Maurin, I.; Guillen, F.; Garcia, A.; Gacoin, T.; Boilot, J.-P. *J. Am. Chem. Soc.* **2010**, *132*, 10967–10969.

(11) Bi, H.; Chen, D.; Li, D.; Yuan, Y.; Xia, D.; Zhang, Z.; Zhang, H.; Wang, Y. *Chem. Commun.* **2011**, *47*, 4135.

(12) Tsukuda, T.; Kawase, M.; Dairiki, A.; Matsumoto, K.; Tsubomura, T. *Chem. Commun.* **2010**, *46*, 1905.

(13) (a) Ni, J.; Zhang, X.; Wu, Y.-H.; Zhang, L.-Y.; Chen, Z.-N. *Chem.—Eur. J.* **2011**, *17*, 1171. (b) Abe, T.; Itakura, T.; Ikeda, N.; Shinozaki, K. *Dalton Trans.* **2009**, 711.

(14) (a) Mizukami, S.; Houjou, H.; Sugaya, K.; Koyama, E.; Tokuhisa, H.; Sasaki, T.; Kanesato, M. *Chem. Mater.* **2005**, *17*, 50. (b) Tzeng, B.-C.; Chang, T.-Y.; Sheu, H.-S. *Chem.—Eur. J.* **2010**, *16*, 9990.

(15) Ni, J.; Zhang, L.-Y.; Wen, H.-M.; Chen, Z.-N. *Chem. Commun.* **2009**, 3801.

(16) Ni, J.; Wu, Y.-H.; Zhang, X.; Li, B.; Zhang, L.-Y.; Chen, Z.-N. *Inorg. Chem.* **2009**, *48*, 10202.

(17) (a) Chan, S.-C.; Chan, M. C. W.; Wang, Y.; Che, C.-M.; Cheung, K. K.; Zhu, N. *Chem.—Eur. J.* **2001**, *7*, 4180. (b) Lu, W.; Chan, M. C. W.; Zhu, N.; Che, C.-M.; He, Z.; Wong, K.-Y. *Chem.—Eur. J.* **2003**, *9*, 6155.

(18) (a) Yam, V. W. W.; Wong, K. M. C.; Zhu, N. *J. Am. Chem. Soc.* **2002**, *124*, 6506. (b) Kato, M.; Omura, A.; Toshikawa, A.; Kishi, S.; Sugimoto, Y. *Angew. Chem., Int. Ed.* **2002**, *41*, 3183.

(19) (a) Hua, F.; Kinayyigit, S.; Cable, J. R.; Castellano, F. N. *Inorg. Chem.* **2005**, *44*, 471. (b) Hissler, M.; Connick, W. B.; Geiger, D. K.; McGarrah, J. E.; Lipa, D.; Lachicotte, R. J.; Eisenberg, R. *Inorg. Chem.* **2000**, *39*, 447. (c) Whittle, C. E.; Weinstein, J. A.; George, M. W.; Schanze, K. S. *Inorg. Chem.* **2001**, *40*, 4053.

(20) (a) Miskowski, V. M.; Houlding, V. H. *Inorg. Chem.* **1991**, *30*, 4446. (b) Hudson, Z. M.; Sun, C.; Harris, K. J.; Lucier, B. E. G.; Schurko, R. W.; Wang, S. N. *Inorg. Chem.* **2011**, *50*, 3447.

(21) Coyer, M. J.; Croft, M.; Chen, J.; Herber, R. H. *Inorg. Chem.* **1992**, *31*, 1752.

(22) Herber, R. H.; Croft; Coyer, M. J.; Bilash, B.; Sahinert, A. *Inorg. Chem.* **1994**, *33*, 2422.

(23) Grosshenny, V.; Romero, F. M.; Ziessel, R. *J. Org. Chem.* **1997**, *62*, 1491.

(24) Sheldrick, G. M. *SHELXL-97: Program for the Refinement of Crystal Structures*; University of Göttingen: Göttingen, Germany, 1997.

(25) Becke, A. D. *J. Chem. Phys.* **1993**, *98*, 5648.

(26) Frisch, M. J.; Trucks, G. W.; Schlegel, H. B.; Scuseria, G. E.; Robb, M. A.; Cheeseman, J. R.; Montgomery, J. A., Jr.; Vreven, T.; Kudin, K. N.; Burant, J. C.; Millam, J. M.; Iyengar, S. S.; Tomasi, J.; Barone, V.; Mennucci, B.; Cossi, M.; Scalmani, G.; Rega, N.; Petersson, G. A.; Nakatsuji, H.; Hada, M.; Ehara, M.; Toyota, K.; Fukuda, R.; Hasegawa, J.; Ishida, M.; Nakajima, T.; Honda, Y.; Kitao, O.; Nakai, H.; Klene, M.; Li, X.; Knox, J. E.; Hratchian, H. P.; Cross, J. B.; Bakken, V.; Adamo, C.; Jaramillo, J.; Gomperts, R.; Stratmann, R. E.; Yazyev, O.; Austin, A. J.; Cammi, R.; Pomelli, C.; Ochterski, J. W.; Ayala, P. Y.; Morokuma, K.; Voth, G. A.; Salvador, P.; Dannenberg, J. J.; Zakrzewski, V. G.; Dapprich, S.; Daniels, A. D.; Strain, M. C.; Farkas, O.; Malick, D. K.; Rabuck, A. D.; Raghavachari, K.; Foresman, J. B.; Ortiz, J. V.; Cui, Q.; Baboul, A. G.; Clifford, S.; Cioslowski, J.; Stefanov, B. B.; Liu, G.; Liashenko, A.; Piskorz, P.; Komaromi, I.; Martin, R. L.; Fox, D. J.; Keith, T.; Al-Laham, M. A.; Peng, C. Y.; Nanayakkara, A.; Challacombe, M.; Gill, P. M. W.; Johnson, B.; Chen, W.; Wong, M. W.; Gonzalez, C.; Pople, J. A. *Gaussian 03*, revision C.02; Gaussian, Inc.: Wallingford, CT, 2004.

(27) Perdew, J. P.; Burke, K.; Ernzerhof, M. *Phys. Rev. Lett.* **1997**, *78*, 3865.

(28) (a) Andrae, D.; Hauessermann, U.; Dolg, M.; Preuss, H. *Theor. Chim. Acta* **1990**, *77*, 123. (b) Schwerdtfeger, P.; Dolg, M.; Schwarz, W. H. E.; Bowmaker, G. A.; Boyd, P. D. W. *J. Chem. Phys.* **1989**, *91*, 1762. (c) Dolg, M.; Wedig, U.; Stoll, H.; Preuss, H. *J. Chem. Phys.* **1987**, *86*, 866.

(29) (a) Pyykkő, P.; Runeberg, N.; Mendizabal, F. *Chem.—Eur. J.* **1997**, *3*, 1451. (b) Pyykkő, P.; Mendizabal, F. *Chem.—Eur. J.* **1997**, *3*, 1458.

(30) Casida, M. E.; Jamorski, C.; Casida, K. C.; Salahub, D. R. *J. Chem. Phys.* **1998**, *108*, 4439.

(31) Stratmann, R. E.; Scuseria, G. E.; Frisch, M. J. *J. Chem. Phys.* **1998**, *109*, 8218.

(32) (a) Cossi, M.; Scalmani, G.; Regar, N.; Barone, V. *J. Chem. Phys.* **2002**, *117*, 43. (b) Barone, V.; Cossi, M. *J. Chem. Phys.* **1997**, *107*, 3210.